Rare Metal Materials and Engineering
Volume 47, Issue 4, April 2018
Online English edition of the Chinese language journal

Available online at www.sciencedirect.com

ScienceDirect

Cite this article as: Rare Metal Materials and Engineering, 2018, 47(4): 1075-1081.

ARTICLE

Enhanced High Temperature Corrosion Resistance of Al_2O_3/Al Composite Coating on γ-TiAl Alloy

Xu Yi, Liang Wenping, Miao Qiang, Wang Ling, Ren Beilei, Cui Shi-yu, Xia Jinjiao, Yao Zhengjun

Nanjing University of Aeronautics and Astronautics, Nanjing 211106, China

Abstract: γ-TiAl specimens were coated with an Al_2O_3/Al composite coating using magnetron sputtering. The corrosion resistance of the coated specimens was investigated in molten salt environment of 100 wt% Na_2SO_4 at 850 °C. Results show that the Al_2O_3/Al composite coating improves the high temperature corrosion resistance of γ-TiAl alloy effectively. The good resistance is attributed to the gradient structure of Al_2O_3/Al composite coating which consists of an Al_2O_3 top-layer, an Al-rich interlayer and a diffusion layer. The results of corrosion test reveal that the Al_2O_3, TiO_2 and $TiAl_3$ are identified as the main phase structure of the corroded coating surface. Moreover, the sealed coating structure could effectively suppress the erosion of O^{2-}, S^{2-} and Na^+, while Al_2O_3/Al coating with gradient structure exhibits superior crack and spallation resistance.

Key words: γ-TiAl; Al_2O_3/Al coating; corrosion resistance; gradient structure

The combination of lower density, high specific strength and excellent high-temperature properties make intermetallic γ-TiAl alloy as the candidate for hot components of advanced aeroengine in the past decades[1-3]. However, the degradation of γ-TiAl alloy in hot corrosion and oxidation environment becomes a significant problem which might limit its further exploitation[4-7].

Surface enhancement plays an important role in improving the environment degradation of γ-TiAl alloy. Among various coating deposition and surface modification techniques, Al, Cr_2O_3 and *M*CrAlY coatings are commonly used to protect γ-TiAl alloy from high temperature oxidation and corrosion[8-10]. These coatings with the distinctive advantages of low cost and high volume production are applicable for a wide range of shapes and sizes without line-of-sight restrictions. However, it has been a common observation that these coatings formed usually contain a large number of micro-cracks running across the whole depth of the coating[11-13]. The micro-cracks are formed during cooling to room temperature as a result of mismatch of thermal expansion coefficients between the coating and the substrate[5,14-16].

In the present paper, an Al_2O_3/Al composite coating with a three-layer structure consisting of an Al_2O_3 top-layer, an Al interlayer and a diffusion zone at the boundary between A1 interlayer and substrate, was introduced on the substrate γ-TiAl alloy. The oxidation resistance of the Al_2O_3/Al composite coating was studied in our past work[17]. Therefore, the aim of this study is to evaluate the corrosion behavior of the Al_2O_3/Al composite coating in fused Na_2SO_4 at 850 °C and try to establish the involved mechanism in the process.

1 Experiment

The γ-TiAl alloy with nominal composition of Ti-46.5A1-4V-1.0Cr (wt%) was used in this study. The substrate specimens, manufactured by Central Iron and Steel Research Institute of China, were produced using powder metallurgy. The dimension of wrought specimen is approximately 15 mm×15 mm×5 mm which was cut by an electric discharge wire cutting machine. The surface was

---

Received date: April 20, 2017
Foundation item: National Natural Science Foundation of China (51474131)

Corresponding author: Liang Wenping, Ph. D., Professor, College of Material Science and Technology, Nanjing University of Aeronautics and Astronautics, Nanjing 211106, P. R. China, Tel: 0086-25-52112626, E-mail: wpliang@nuaa.edu.cn

ground down and polished roughly, and then cleaned ultrasonically in ethanol and dried prior to tests.

The Al_2O_3/Al composite coatings were fabricated in a magnetron sputtering system. An aluminum plate with a purity of 99.99% prepared by powder metallurgy was used as the sputtering target. Pure Ar and O_2 were used as the working and reactive gases, respectively. The Al_2O_3/Al composite coating was deposited in two steps, Al deposition and Al_2O_3 reactive deposition, using the set-up parameters in Table 1. After deposition, the coated specimens were heat treated in a vacuum furnace (10^{-4} Pa) at 600 °C for 10 h before corrosion test.

Adhesion strength of the Al_2O_3/Al composite coatings on γ-TiAl were measured by a scratch tester (WS-2006), equipped with a 200 μm radius Rockwell diamond indenter, which was drawn across the coatings surfaces using a linearly increased normal load from 0 N to 100 N. The rate of load increase was set at 20 N/min and the speed of indenter was 2 mm/min. The scratch length was 10 mm. An AE sensor was attached near the diamond indenter to detect the acoustic signals emitted from the coating failure. The minimum load at which coating failure occurs is defined as the critical load (L_C) and represents an indication of the coating adhesion.

The substrate and Al_2O_3/Al coated samples were placed in the alumina crucibles filled with a supersaturated solution of high purity Na_2SO_4 (>99.9 wt%). The test contained 10 cycles. For each cycle, the samples were kept in a furnace at 850 °C in static air for 10 h and rapidly cooled to room temperature. The mass gain (sample+crucible+Na_2SO_4 salt) was weighed by an electronic balance with sensitivity of 10^{-5} g. After the measurement, the samples were placed in the alumina crucibles filled with the high purity Na_2SO_4 and then put back to continue the next cycle. For every experiment, three samples were used in the same condition to get the average mass change. After the test, the samples were only used cotton bar and soft brush to clean up the salt in order to keep the original morphologies of samples.

The phase composition of deposited coatings after oxidation at different temperatures was identified by X-ray diffraction (XRD, BurkerD8 ADVANCED, Cu Kα source radiation). The morphologies and chemical compositions of coatings and oxide scales were observed and determined by a scanning electron microscope (SEM, Quanta200, FEI Company) equipped with an energy-dispersive spectrum (EDS, XMS60S).

Table 1 Deposition parameters of Al_2O_3/Al reactive sputtering

Parameters	Al layer	Al_2O_3 layer
Power/W	150	250
Voltage/V	700	1000
Working pressure/Pa	0.5	0.5
Ar/mL·min^{-1}	30	50
O_2/mL·min^{-1}	0	6
Target to substrate distance/mm	30	30
Diffusion time/h	3	5
Sample temperature/°C	250	300

2 Results

2.1 Microstructure of as-deposited coating

Fig.1a shows the virgin surface of the as-deposited Al_2O_3/Al coating by magnetron sputtering. It can be found that the coating is very uniform with a low occurrence of major growth defects. This is also proved by the low surface roughness value (0.143 μm), measured by Roughness Tester (TR210, Shanghai Lingyi Company, China). The EDS result of coating surface indicates that the O element is about 1.5 times the atom content of Al element, as shown in Fig.1b. The SEM and EDS cross-section of coating, as shown in Fig.1c, 1d respectively, illustrate a dense composite layers structure with a thickness of ~20 μm which consists of an Al_2O_3 top-layer, an Al interlayer and a diffusion layer (the diffusion layer was formed during the coating deposition). It also clearly depicts good interface bonding between the top-layer/interlayer and interlayer/substrate.

The phase structure of Al_2O_3/Al composite coating consists of α-Al_2O_3 (JCPDS NO. 84-1468) and Al (JCPDS NO. 04-0787), as shown in Fig.2, which accords with the EDS results of the coating.

2.2 Scratch test results

As one of the main quality indicators, the coating adhesion strength was determined by the scratch test. The critical load on the substrate with the coating starts to be visible according to the acoustic signal when it is captured at the beginning of the occurrence of coating failure during the scratch test. The acoustic emission curves are plotted as a function of the normal load in Fig.3a and the corresponding scratch morphology is displayed in Fig.3b. The critical load of Al_2O_3/Al coating on γ-TiAl alloy is 50 N, above which the adhesion strength between the coating and substrate is generally sufficient for applications[18,19]. The evidence of plastic deformation can be seen in the scratch track of Al_2O_3/Al coating which indicates good adhesion strength between the coating and the substrate.

2.3 Results of hot corrosion test

2.3.1 Microstructure of specimens after hot corrosion test

The photos of the substrates and Al_2O_3/Al coated samples after 100 h corrosion at 850 °C are presented in Fig.4. It can be found that the corrosion scales of substrate turn white to tawny with the test time increasing. The corrosion scales have already spalled from the substrate continuously which indicates the poor corrosion resistance of the substrate γ-TiAl alloy. On the other hand, the Al_2O_3/Al coating remains intact even after 100 h at 850 °C in Na_2SO_4 fused salt. The color of Al_2O_3/Al coating turns silver to taupe. No evidences of coating degradation can be found in these macroscopical photos.

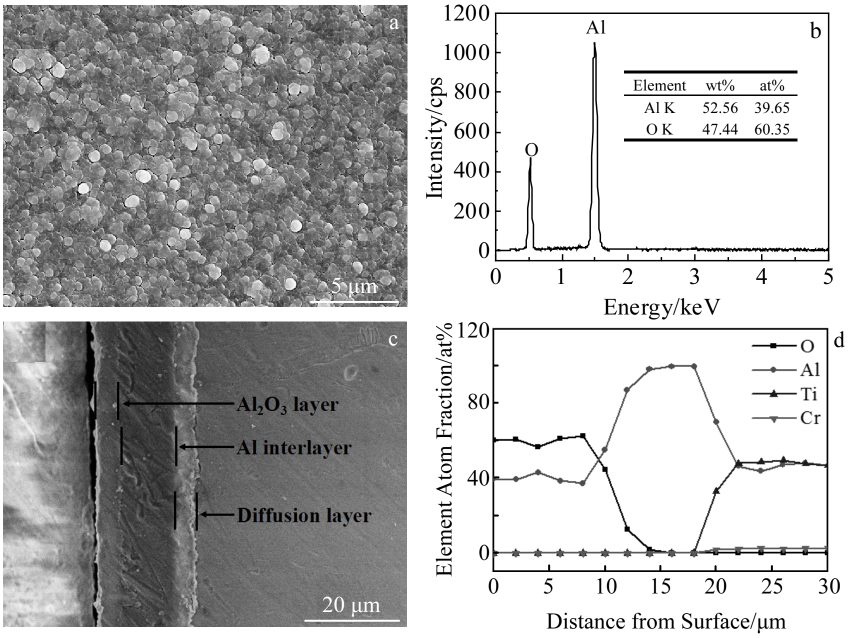

Element	wt%	at%
Al K	52.56	39.65
O K	47.44	60.35

Fig.1 Surface image (a), EDS result (b), cross-section image (c) and line scanning result (d) of Al_2O_3/Al composite coating

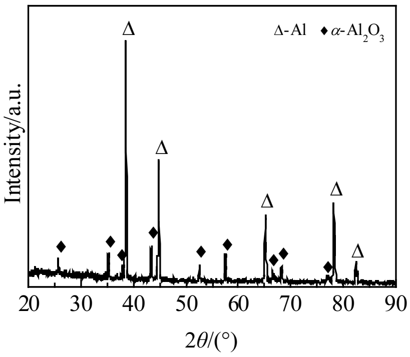

Fig.2 XRD pattern of Al_2O_3/Al composite coating on γ-TiAl alloy before oxidation test

Fig.5 shows the surface morphologies and the corresponding EDS results of the substrate and the Al_2O_3/Al coating after corrosion test. The corroded substrate displays a massive structure surface appearance, as shown in Fig.5a, while the needle-like structure appearance can be found in the surface of the corroded coating in Fig.5c. A large amount of O element (63.97 at%) can be detected in the surface of the corroded substrate in Fig.5b, indicating that oxidation is the main reaction of substrate during the corrosion test. Similar content of O element (57.64 at%) can be detected in the surface of the corroded coating. A considerable amount of Na and S elements (25.06 and 13.40 at%, respectively) can also be detected which is contributed by the fused Na_2SO_4.

Fig.6 shows the cross-section morphologies and the corresponding EDS line-scan of substrate and the Al_2O_3/Al coating after corrosion test, which were measured from the top surface to the interior. The corroded scale spalls from the substrate continuously during the corrosion test, and the corroded substrate shows a cross-section with multilayer structure

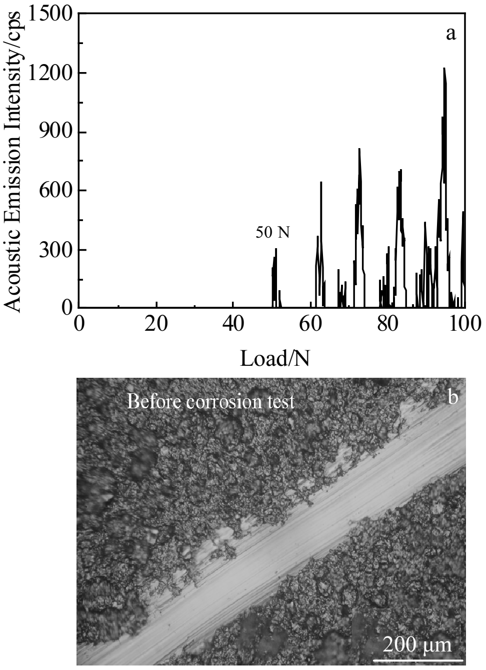

Fig.3 Sound emission peaks against the applied load according to the scratch test on Al_2O_3/Al composite coating (a) and the corresponding scratch morphology (b)

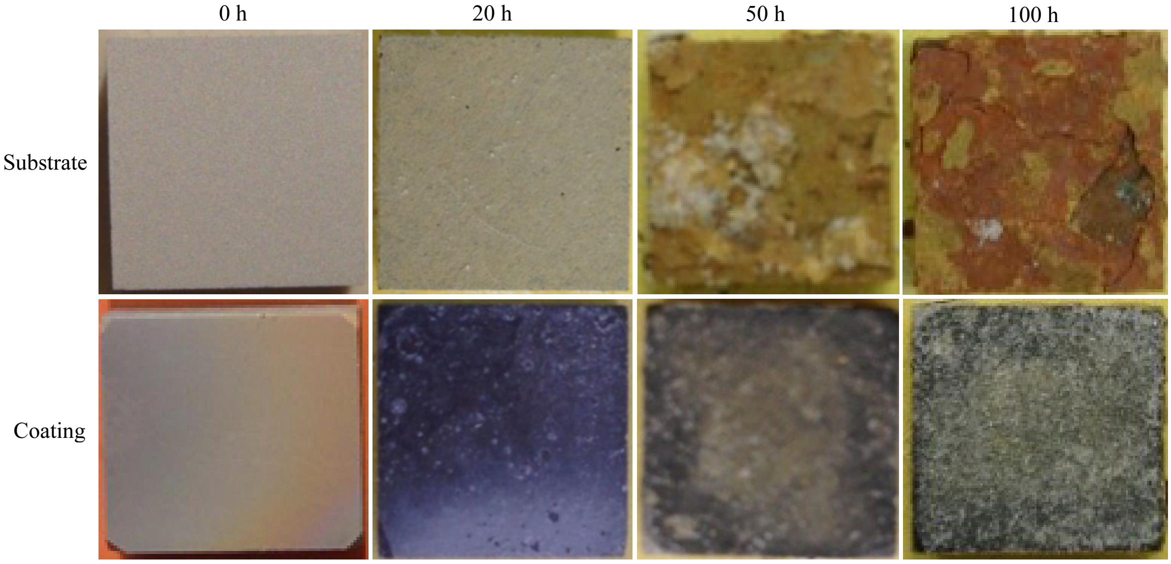

Fig.4 Macroscopical images of the samples without and with the Al_2O_3/Al composite coating during the corrosion test at 850 °C

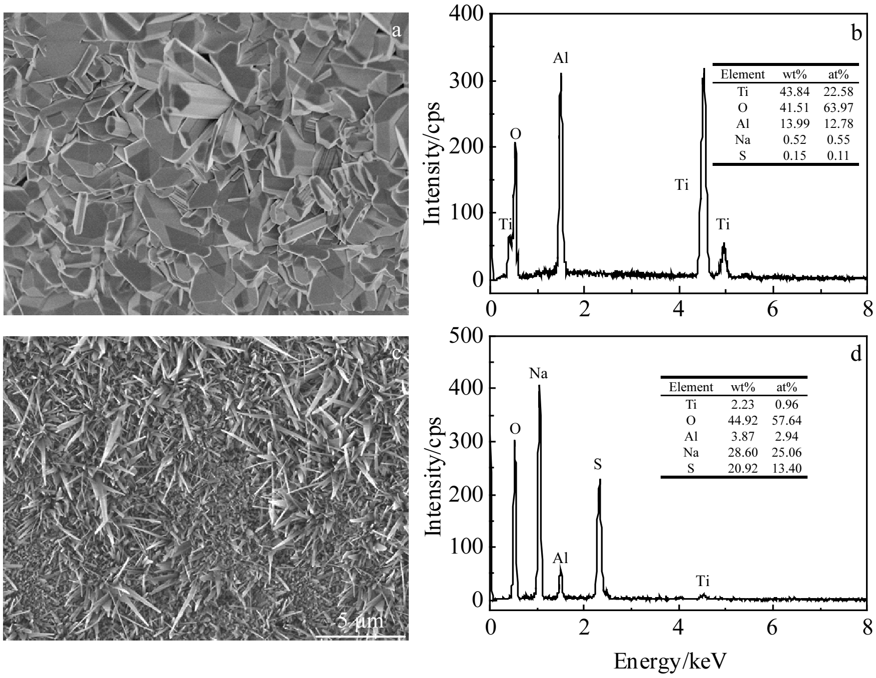

Element	wt%	at%
Ti	43.84	22.58
O	41.51	63.97
Al	13.99	12.78
Na	0.52	0.55
S	0.15	0.11

Element	wt%	at%
Ti	2.23	0.96
O	44.92	57.64
Al	3.87	2.94
Na	28.60	25.06
S	20.92	13.40

Fig.5 Surface morphologies (a, c) and EDS results (b, d) of substrate γ-TiAl alloy (a, b) and Al_2O_3/Al composite coating (c, d) after 850 °C hot corrosion test

which is resulted from the Na_2SO_4 erosion in Fig.6a. However, the corroded coating is still compact and unbroken as well as no though-wall cracks and pores can be found in the cross-section, as shown in Fig.6c.

Fig.7 shows the XRD patterns of the substrate and the Al_2O_3/Al coating after corrosion test. Al_2O_3, TiO_2 and $TiAl_3$ are identified as the main phase structure of the coating surface after the corrosion test, while the Al_2O_3 and TiO_2 to the substrate. The Na_2SO_4 phase which is adsorbed on the sample surface can be detected in both coating and substrate surface obviously.

2.3.2 Hot corrosion kinetics

The kinetics curve of the coated samples after 100 h corrosion at 850 °C was plotted with substrate as comparison, as shown in Fig.8. The mass gain of the substrate is larger than that of the coated sample during the whole test. On the other hand, the Al_2O_3/Al composite coating maintains their integrity with no detectable sign of scale spallation or crack during the

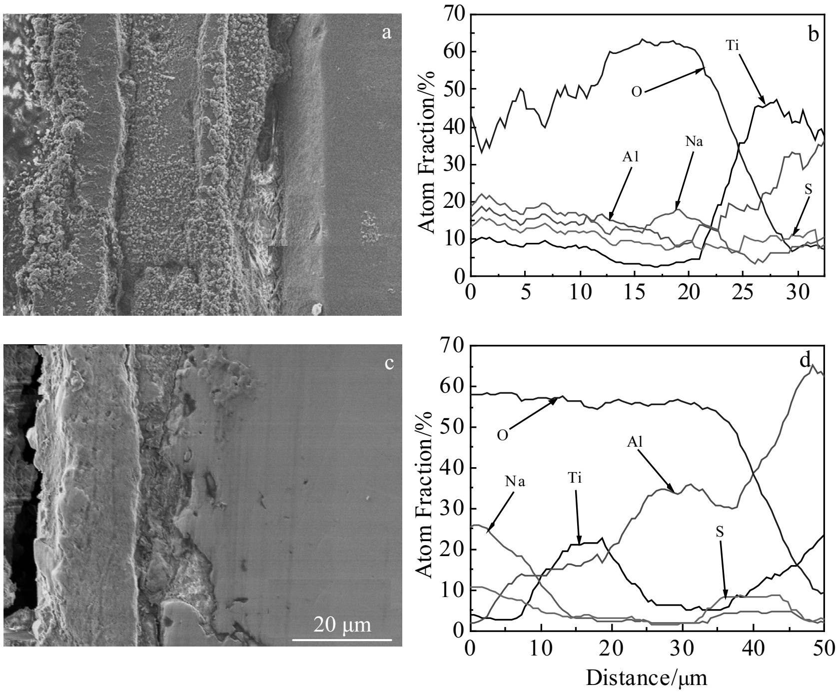

Fig.6 Cross-section morphologies (a, c) and EDS line scan results (b, d) of substrate γ-TiAl alloy (a, b) and Al_2O_3/Al composite coating (c, d) after 850 °C hot corrosion test

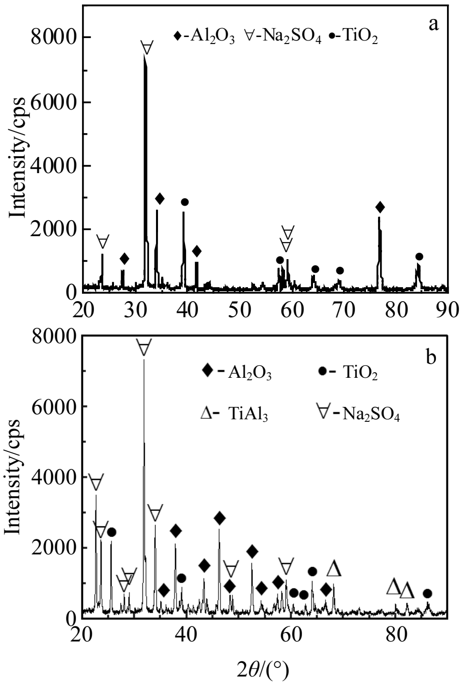

Fig.7 XRD patterns of substrate γ-TiAl alloy (a) and Al_2O_3/Al composite coating (b) after 850 °C hot corrosion test

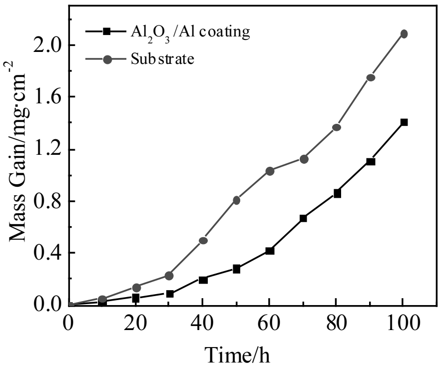

Fig.8 Mass change vs time for substrate γ-TiAl alloy and Al_2O_3/Al composite coating during hot corrosion at 850 °C

entire corrosion period of 100 h, suggesting that it can effectively enhance the corrosion resistance of the substrate through the formation of a more stable and adherent corrosion scale. The mass gain of Al_2O_3/Al composite coating after 100 h corrosion test is 1.409 mg/cm^2, which is an optimism value.

3 Discussion

3.1 Corrosion mechanisms of substrate

The corrosion and oxidation resistance of the substrates mainly depends on the integrality of protective coatings. In this study, the processes of protective coating cracking and spallation are the key factor to influence the lifetime of γ-TiAl and the prepared protective coating[20-23].

The fused salt on the surface usually induces two types of hot corrosion: type I, named high temperature corrosion, at temperature within 825~925 °C and type II, named low temperature corrosion, at temperature below 825 °C[22,24-26]. Both the two corrosion types will lead to the depletion of beneficial elements, internal sulfidation and oxidation, even severer failure of coating system. In the present study, the samples were exposed in Na_2SO_4 at 850 °C, which is lower than the melt point of the salt (884 °C). In order to avoid the damage of the original appearance, the samples were cleaned by cotton bar not in de-ionized water to get rid of the salt clearly after every cycle. It means a large number of Na_2SO_4 and Na_2SO_3 remnant on the sample surface after the experiment.

In the fused salts, the following reactions took place:

$$2SO_4^{2-}=2SO_3^{2-}+O_2 \tag{1}$$

$$Ti^{2+}+O^{2-}=TiO \tag{2}$$

$$Ti^{4+}+2O^{2-}=TiO_2 \tag{3}$$

$$2Al^{3+}+3O^{2-}=Al_2O_3 \tag{4}$$

There is a competition among the elements for oxidation since some of the oxides are more stable than others. As a result of this competition, there is a tendency for the coating to become covered with the most thermodynamically stable oxide which is called selective oxidation. Al and Ti will react with the oxygen to form alumina and titanium oxide, respectively. In comparison to titanium oxide, alumina has the lowest free energy of formation and is easy to be produced during exposure at 850 °C thermodynamically, but Ti has lower activity but higher diffusion rate than Al. At this high temperature, Ti diffuses outward fast and selective oxidation of Ti occurs, and is oxidized to TiO_2 and the growth rate of TiO_2 is great. The TiO_2 with a loose and porous structure may weaken the protective coating[27-29]. Therefore, the loose layer in the substrate surface contains not only alumina but also titanium oxide. It implies more Ti enters into the surface layer by outward diffusion and forms loose and porous TiO_2, as shown in Fig.9a. As a result, the newly formed porous Al_2O_3 cannot play a crucial role in protecting the coating. Ti oxides produced by reaction can destroy the oxide scale gradually. Thus, the occurrence of TiO_2 is indicative for the fact that the coating is destroyed. The major role of the salt in hot corrosion is to crack or break the protective oxide scale as well as to produce the internal void. With the progress of the corrosion, some cracks are formed due to plastic deformation and grain growth. O^{2-}, S^{2-} and Na^+ present at the cross-section lead to porosity and sponginess and cause the formation of internal oxide. Oxygen molecules could penetrate into the scale along various paths, such as grain boundaries, pores, cracks and defects.

3.2 Corrosion mechanisms of Al_2O_3/Al coated sample

Compared with the substrates, the coated samples reveal good stability in the fused salt of Na_2SO_4. Alumina is an oxide ceramic that possesses a stubborn chemical stability besides high strength and high rigidity, even at elevated temperatures. As shown in Fig.9b, the sealed coating structure can effectively suppress the erosion of O^{2-}, S^{2-} and Na^+ owing to the excellent inertness of Al_2O_3/Al coating in fused salts.

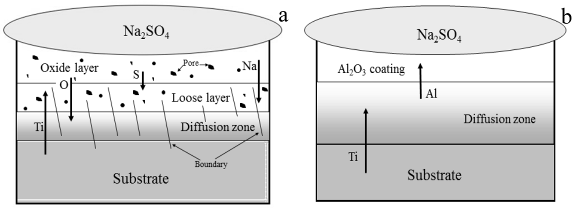

Fig.9 Schematic diagrams of *γ*-TiAl alloy (a) and Al_2O_3/Al composite coating (b) evolution during corrosion test at 850 °C

On the other hand, the Al_2O_3/Al composite coating has superior crack and spallation resistance because of its gradient structure. The outward and inward diffusion of the Al element from interlayer leads to a gradient section structure of the coating system. Meanwhile, the Al interlayer provides sufficient Al source for the formation of a continuous Al_2O_3 layer in the coating surface. Increasing the test time, the Al interlayer is exhausted, while the thickness of intermediate diffusion layer grows, as shown in Fig.9b. Thus, the presence of an Al interlayer assures the beneficial effect of a stable and compact Al_2O_3 layer. The outward diffusion of Ti was detected by EDS and XRD techniques during oxidation test, as shown in Fig.6 and Fig.7. As an active intermetallic element with Ti, Al suppresses the out diffusion of Ti to the coating surface effectively because of the synthesis of Ti-Al intermetallics, such as $TiAl_2$, $TiAl_3$.

4 Conclusions

1) The as-deposited Al_2O_3/Al composite coating which consists of an Al_2O_3 top-layer, an Al interlayer and a diffusion layer is compact, uniform and has good adhesion with substrate *γ*-TiAl alloy.

2) The Al_2O_3/Al composite coating with a thickness of ~20 μm provides excellent corrosion resistance in 850 °C fused Na_2SO_4 for 100 h. The coating is intact and the average mass gain of coated samples is less than that of the substrate.

3) Al_2O_3, TiO_2 and $TiAl_3$ are identified as the main phase structure of the coating surface after the corrosion test, while the Al_2O_3/Al composite coating transforms to an oxide top-layer and a Ti-Al diffusion interlayer.

4) The Al_2O_3/Al composite coating has superior crack and spallation resistance because of its gradient structure, while the sealed coating structure can effectively suppress the erosion of O^{2-}, S^{2-} and Na^+ owing to the excellent inertness of Al_2O_3/Al coating in fused salts.

References

1 Bauer V, Christ H J. *Intermetallics*[J], 2009, 17(5): 370
2 Chen W R, Beddoes J, Zhao L. *Materials Science and*

Engineering A[J], 2002, 323(1-2): 306

3 Liu X P, Ge P Y, You K *et al. Rare Metal Materials and Engineering*[J], 2011, 40(11): 1891

4 Du H L, Aljarany A, Datta P K *et al. Corrosion Science*[J], 2005, 47(7): 1706

5 Xi Y J, Liu Y J, Lu J B *et al. Rare Metal Materials and Engineering*[J], 2008, 37(12): 2165 (in Chinese)

6 Xu Y, Miao Q, Liang W P *et al. Rare Metal Materials and Engineering*[J], 2014, 43(11): 2652

7 Lavrenko V A, Panasyuk A D, Firstov S A *et al. Powder Metallurgy and Metal Ceramics*[J], 2003, 42(3-4): 184

8 Zhang P, Guo X P. *Corrosion Science*[J], 2013, 71: 10

9 Cheng Y X, Wang W, Zhu S L *et al. Intermetallics*[J], 2010, 18(4): 736

10 Tang Z L, Wang F H, Wu W T. *Surface and Coatings Technology*[J], 1998, 99(3): 248

11 Tang Z L, Wang F H, Wu W T. *Surface and Coatings Technology*[J], 1998, 110(1-2): 57

12 He Z Y, Wang Z X, Zhang F *et al. Surface and Coatings Technology*[J], 2013, 228(S1): 287

13 Zhou C G, Xu H B, Gong S K *et al. Surface and Coatings Technology*[J], 2000, 132(2-3): 117

14 Ai T T, Wang F, Feng X M. *International Journal of Minerals Metallurgy and Materials*[J], 2009, 16(3): 339

15 Braun R, Lange A, Hovsepian P E *et al. Materials at High Temperatures*[J], 2011, 28(4): 324

16 Ma X X, He Y D, Lin J P *et al. Surface and Coatings Technology*[J], 2012, 206(10): 2690

17 Xu Y, Liang W P, Miao Q *et al. Surface Engineering*[J], 2015, 31(5): 354

18 Ma X, Matthews A. *Surface and Coatings Technology*[J], 2007, 202(4-7): 1214

19 Xu Y, Miao Q, Liang W P *et al. Surface Engineering*[J], 2014, 30(1): 64

20 Tang Z L, Wang F H, Wu W T. *Intermetallics*[J], 1999, 7(11): 1271

21 Das S, Datta S, Basu D *et al. Ceramics International*[J], 2008, 34(5): 1215

22 Yao J Q, He Y D, Wang D R *et al. Corrosion Science*[J], 2014, 80: 19

23 Yu C Z, Zhu S L, Wei D Z *et al. Surface and Coatings Technology*[J], 2007, 201(16-17): 7530

24 Eliaz N, Shemesh G, Latanision R M. *Engineering Failure Analysis*[J], 2002, 9(1): 31

25 Katsman A, Ginzburg A, Werber T *et al. Surface and Coatings Technology*[J], 2000, 127(2-3): 219

26 Menzies I A, Hill D L, Hills G J *et al. Journal of Electroanalytical Chemistry*[J], 1959, 1(2): 161

27 Knutsson P, Lai H, Stiller K. *Corrosion Science*[J], 2013, 73: 230

28 Chuprina V G, Shalya I M. *Powder Metallurgy and Metal Ceramics*[J], 2007, 46(11-12): 582

29 Dong Z Q, Jiang H R, Feng X R *et al. Transactions of Nonferrous Metals Society of China*[J], 2006, 16(S3): 2004

γ-TiAl 合金表面 Al_2O_3/Al 复合涂层的抗高温熔盐腐蚀性能

徐 一，梁文萍，缪 强，王 玲，任蓓蕾，崔世宇，夏金姣，姚正军
(南京航空航天大学，江苏 南京 211106)

摘　要：采用磁控溅射技术于 *γ*-TiAl 合金表面制备 Al_2O_3/Al 复合涂层。在 850 ℃下、100%（质量分数）Na_2SO_4熔盐中观测 Al_2O_3/Al 复合涂层的高温腐蚀行为。结果表明，Al_2O_3/Al 复合涂层具备由 Al_2O_3 表层、富 Al 中间层以及互扩散层组成的梯度结构，因而有效地提高了基体 *γ*-TiAl 合金的抗高温腐蚀性能。在腐蚀实验后，涂层试样表面相结构为 Al_2O_3、TiO_2 和 $TiAl_3$。致密的 Al_2O_3/Al 复合涂层有效地抑制了 O^{2-}、S^{2-}和 Na^+对基体 *γ*-TiAl 合金的侵蚀。并且，Al_2O_3/Al 复合涂层的梯度结构亦使其表现出了优异的抗开裂和抗剥落性能。

关键词：*γ*-TiAl 合金；Al_2O_3/Al 复合涂层；抗熔盐腐蚀；梯度结构

作者简介：徐 一，男，1986 年生，博士生，南京航空航天大学材料科学与技术学院，江苏 南京 211106，电话：025-52112626，E-mail: nuaaxuyi@163.com